NASA TECHNICAL MEMORANDUM

NASA TM X-2549

NASA TM X-2549

EXPERIMENTAL INVESTIGATION OF CIRCULAR, FLAT, GROOVED AND PLAIN STEEL DIAPHRAGMS BURSTING INTO A 30.5-CENTIMETER-SQUARE SECTION

by Yoshio Yamaki and James R. Rooker

Langley Research Center
Hampton, Va. 23365

NATIONAL AERONAUTICS AND SPACE ADMINISTRATION • WASHINGTON, D. C. • MAY 1972

1. Report No.	2. Government Accession No.	3. Recipient's Catalog No.
NASA TM X-2549		

4. Title and Subtitle	5. Report Date
EXPERIMENTAL INVESTIGATION OF CIRCULAR, FLAT, GROOVED AND PLAIN STEEL DIAPHRAGMS BURSTING INTO A 30.5-CENTIMETER-SQUARE SECTION	May 1972
	6. Performing Organization Code

7. Author(s)	8. Performing Organization Report No.
Yoshio Yamaki and James R. Rooker	L-4645
	10. Work Unit No.
9. Performing Organization Name and Address	117-07-04-09
NASA Langley Research Center Hampton, Va. 23365	11. Contract or Grant No.
	13. Type of Report and Period Covered
12. Sponsoring Agency Name and Address	Technical Memorandum
National Aeronautics and Space Administration Washington, D.C. 20546	14. Sponsoring Agency Code

15. Supplementary Notes

16. Abstract

Limited data on the bursting of circular, initially flat, grooved and plain steel diaphragms opening into a 30.5-cm-square section are presented in tabular form. In addition, these data were used to determine values of an empirical constant to be used in a design equation for predicting diaphragm bursting pressures and opening times.

17. Key Words (Suggested by Author(s))	18. Distribution Statement
High-pressure diaphragms Shock tube diaphragm Diaphragm opening technique	Unclassified – Unlimited

19. Security Classif. (of this report)	20. Security Classif. (of this page)	21. No. of Pages	22. Price*
Unclassified	Unclassified	29	$3.00

*For sale by the National Technical Information Service, Springfield, Virginia 22151

EXPERIMENTAL INVESTIGATION OF CIRCULAR, FLAT, GROOVED AND PLAIN STEEL DIAPHRAGMS BURSTING INTO A 30.5-CENTIMETER-SQUARE SECTION

By Yoshio Yamaki and James R. Rooker
Langley Research Center

SUMMARY

Limited data on the bursting of circular, initially flat, grooved and plain steel diaphragms opening into a 30.5-cm-square section are presented in tabular form. The parameters considered are the following: diaphragm thickness, diaphragm hardness, material ultimate strength, groove depth, and rate of pressure rise. From these data, the dimensions for five diaphragms which will burst at 6.9 MN/m^2 increments from 6.9 to 34.5 MN/m^2 were selected for use in a proposed 30.5-cm-square shock tube. In addition, these data were used to determine values of an empirical constant to be used in a design equation for predicting diaphragm bursting pressures and opening times. Design equations are plotted along with the respective data for steel diaphragms with material ultimate strengths of 517.1, 558.5, and 634.3 MN/m^2. Seventy-two percent of the burst-pressure data and thirty-eight percent of the opening-time data fall within ±10 percent of the empirical curves. The average error for the predicted burst pressure was 7.8 percent and that for the predicted opening time was 14 percent; however, the validity of the equations has been established only for the sizes tested. Burst pressures range from 3.5 to 34.5 MN/m^2. Also briefly discussed are the opening times for knife-sheared diaphragms, and the effects of groove geometry and opening bend radius on diaphragm-bursting characteristics.

INTRODUCTION

The proposed construction of an impulse facility at Langley Research Center which would operate in the pressure range of 6.9 to 34.5 MN/m^2 required the determination of the bursting characteristics of a diaphragm spanning a 30.5-cm opening. Diaphragm-bursting characteristics have been the subject of several previous investigations. In reference 1 Rast investigated circular metal diaphragms bursting into circular openings with diameters between 2.54 and 13.41 cm and in reference 2 Armstrong and Watson investigated circular diaphragms bursting into a 5-cm-square cross section. References 3 to 5 were concerned with the measurement of opening times for diaphragms

bursting into rectangular cross sections which were less than 15 cm. However, no information was available concerning the design of steel diaphragms bursting into 30.5-cm-square openings at the pressures of interest; therefore, a diaphragm test program was undertaken in a facility constructed for this purpose.

The primary objective of this diaphragm test program was to find easily constructed diaphragms that would burst reliably with no fragmentation at 6.9, 13.8, 20.7, 27.6, and 34.5 MN/m^2. In addition, these diaphragms were to have quick opening times in order to minimize shock formation distance. Thus, plain, shallow-grooved, and knife-sheared diaphragms were tested in a pressure range from 3.5 to 34.5 MN/m^2 with a pressure rise rate between 0.05 MN/m^2-sec and 483 MN/m^2-sec. The diaphragms were fabricated from AISI 1010 steel, AISI 4130 steel, and AISI 347 stainless steel in commercial thicknesses ranging from 1.6 to 6.4 mm. The ratio of the diaphragm thickness at the groove root to plate thickness ranged from 0.87 to 1.00, and two groove geometries were tested. The opening bend radius, which was located on the square section of the transition head in order to provide a rounded edge for the diaphragm petals to bend over during the opening sequence, was varied from 3.2 to 19.1 mm.

SYMBOLS

Measurements and calculations were made in the U.S. Customary Units. They are presented herein in the International System of Units (SI).

C_0, C_1, C_2, C_3	dimensionless constants for polynomial equation
h	maximum diaphragm deflection, centimeters
K	dimensionless constant for burst-pressure equation
p	pressure, meganewtons per square meter gage
R_B	Rockwell hardness for B scale
r	hydraulic radius of unsupported area of diaphragm, centimeters
r_o	radius of sphere, centimeters
r_s	root radius, millimeters

S dimensionless parameter defined as $\frac{4}{\frac{h}{r}+\frac{r}{h}}$

t diaphragm thickness, millimeters

t_s diaphragm thickness at groove root, millimeters

θ time, seconds

ρ diaphragm material density, kilograms per cubic meter

σ ultimate tensile stress of diaphragm material, meganewtons per square meter

ϕ dimensionless burst-pressure factor used in reference 6

DESCRIPTION OF APPARATUS

A typical diaphragm is shown in figure 1. The diaphragms were fabricated from commercial sheets and plates with standard mill finishes and were not checked for internal flaws. Nominal thicknesses of 1.6, 2.4, 3.2, 4.8, and 6.4 mm were used. Figure 2 shows the groove geometries tested. The diaphragms were clamped on a milling machine and a circular saw blade was used to cut a cross pattern. A micrometer dial indicator was used to survey the groove depth at the center and along each arm of the pattern. The groove depth was established as the average of the maximum and minimum readings. Diaphragms with variations of groove depth which were judged to be unreasonable were rejected. A mild steel ring was welded to the diaphragm to help retain it in the test fixture. Preliminary tests of diaphragms without this ring indicated that the diaphragms would pull in from the clamped edges as a result of bolt elongation during the pressurization. The welding was done after the machining because the welding produced some diaphragm distortion. Early tests of the diaphragm with the ring indicated that the weld bead should be at least equal to the diaphragm thickness in order to prevent the shearing of the ring from the diaphragm.

Figure 3 shows the diaphragm clamping arrangement which consisted of three stainless-steel parts: driver chamber, floating head, and transition head. The driver chamber was 1.8 m long with a 33.0-cm inside diameter. The floating head maintained the chamber seal during the elongation of the bolts; the transition head provided a square cross section so that the diaphragm petals would bend along a straight line during the opening sequence. The initial opening bend radius was 3.2 mm, and later increased to 6.4 and 19.1 mm.

In order to obtain pressure rise rates between 0.05 and 483 MN/m^2-sec, two different pressurizing techniques were utilized. Pressure rise rates between 0.05 and 0.1 MN/m^2-sec were obtained by controlling a hand-operated valve. The pressure rise rate for two positions of the valve (open, half open) was determined with the use of a timer. The instrumentation for this pressurizing technique is shown in figure 4. The pressure gage port was located in the wall of the driver chamber 81 cm upstream of the diaphragm. The diaphragm's maximum deflection was measured by the bulge height indicator which consisted of an aluminum rod perpendicular to and in contact with the diaphragm. Movement of this rod in relation to a stationary rule was recorded by a 16-mm camera operating at 16 frames per second. This camera also recorded the pressure gage reading. A second high-speed 16-mm camera (6600 frames/second) recorded the opening sequence from which the diaphragm opening time was determined.

Pressure rise rates between 0.1 and 483 MN/m^2-sec were obtained by pressurizing the driver chamber until the deflecting diaphragm contacted a preset probe which started the ignition of 250 grams of smokeless powder with a typical burning time of 15 milliseconds. Setting of the probe was on the basis of 90 percent of the deflection known to cause burst in the previous test. The instrumentation for this diaphragm test is shown in figure 5. Since the explosive charge was expected to yield a nonuniform pressure distribution and a rapid pressure fluctuation, three pressure transducers with response rates of 60 000 Hz per second were located 5, 71, and 142 cm upstream of the diaphragm. A high-speed strip chart recorder with the same response rate recorded the output of the transducers, and a 16-mm camera, operating at 6000 to 7000 frames per second, was actuated along with the powder ignition to record the diaphragm opening. An electrical probe was located on the transition head wall to indicate when the diaphragm petals touched the wall, and the probe signal was recorded by the strip chart recorder. Four times during the test program the pressure instrumentation was calibrated by applying the pressure from a deadweight tester to the chamber.

A fixed stainless-steel knife, which is shown in figure 6, was used to rupture a few plain diaphragms. Diaphragm rupture was initiated when the deflecting diaphragm struck the piercer in the center of the knife, and then the diaphragm was sheared into four petals by the knife blades. Position of the knife was fixed at 4.4 cm downstream of the diaphragm.

RESULTS AND DISCUSSION

Effect of Groove Geometry

The data from the plain and grooved diaphragm test are presented in table I. All but nine of these grooved diaphragms were cut with a V-groove with a 0.25-mm root radius.

Six of these nine diaphragms were cut with a V-groove with the root radius varying between 0.50 and 2.00 mm in order to investigate the effect of root radius on burst pressure. Data for these diaphragms are presented in table II along with data for two V-grooved diaphragms with 0.25-mm root radii. There is no significant change in burst pressure with root radius. This result indicates that a 0.25-mm root radius is large enough to minimize the effects of stress concentration associated with the V-groove. The other three diaphragms were cut with a 1.6-mm-wide groove in order to investigate the effect of groove geometry on burst pattern. The fracture line for these diaphragms jumped across the wide groove from corner to corner as the crack propagated along the groove pattern. This shearing resulted in jagged edges which could cause petal fragmentations; therefore, this geometry was discontinued. Plain diaphragms and grooved diaphragms with t_s/t ratios larger than 0.96 also experienced jagged breaks and petal fragmentation during burst. In figure 7 two ruptured diaphragms, one grooved and one plain, are shown to illustrate this effect.

Knifed Diaphragms

The data for plain diaphragms that were ruptured with the knife are presented in table III. Included in this table are burst-pressure data from table I for grooved diaphragms bursting at approximately the same pressures. There are no opening times available for three of the eleven knife-sheared diaphragms and no comparable data from table I for another knife-sheared diaphragm. However, these limited data indicate that the opening times for knife-sheared diaphragms are longer than those for grooved diaphragms bursting at the same pressures.

Effect of Bend Radius

The initial 3.2-mm opening bend radius located on the transition head resulted in the diaphragm petals being sheared off at their bases. An increase in the opening bend radius to 6.4 mm was satisfactory for diaphragm thicknesses up to 3.2 mm; however, an increase to 19.1 mm was required in order to prevent this petal shear failure of the thicker diaphragms. Therefore, an opening bend radius that is at least three times the maximum diaphragm thickness is recommended to prevent this petal shear failure.

Effect of Pressure Rise Rate

The effect of pressure rise rate was not apparent from the limited data; however, these data are included in table I. The burst pressures given in table I for diaphragms subjected to pressure rise rates between 0.1 MN/m^2-sec and 483 MN/m^2-sec are the pressures recorded by the transducer closest to the diaphragm.

Effect of Work Hardening

Also included in table I are the data for three diaphragms fabricated from normalized AISI 4130 steel. These diaphragms sheared satisfactorily into four petals, but their petals also broke completely off along their base. This problem was not encountered when the annealed 4130 steel diaphragms were tested. The normalizing process results in the petal having a higher hardness than that in the annealed state. Therefore, a possible explanation would be that the diaphragm petals work hardened during the opening process and a brittle fracture resulted. Further testing of diaphragms fabricated from normalized 4130 steel was discontinued since petal fragmentation was not allowed.

Correlating Equation

In order to correlate the test data in table I, an empirical constant K was determined for each material tested. This constant would be used in the equations to predict the burst pressure and opening times:

$$p = \frac{Kt_s\sigma}{r} \tag{1}$$

$$\theta = \sqrt{\frac{\pi\rho rt}{4p}} \tag{2}$$

Substituting equation (1) into equation (2) yields

$$\theta = \sqrt{\frac{\pi\rho r^2 t}{4Kt_s\sigma}} \tag{2a}$$

The origins of equations (1) and (2) and the method for formulating the empirical constants are discussed in the appendix. The resulting form for the empirical constant within the limiting range of t_s/t is

$$K = \left[C_3(t_s/t)^3 + C_2(t_s/t)^2 + C_1(t_s/t) + C_0\right] \tag{3}$$

where C_3, C_2, C_1, and C_0 depend on the diaphragm material. Values for these constants for the three materials tested are given in table IV and a plot of K for t_s/t values ranging from 0.87 to 1.00 is presented in figure 8 for each material. Values for K are given in table V. This plot indicates that of the three materials tested, AISI 347 stainless steel is the least sensitive to the thickness ratio parameter. This characteristic in combination with the higher ultimate strength of AISI 347 stainless steel makes it a more

suitable material for diaphragms. This characteristic is denoted in equation (2a) where the opening time is inversely proportional to ultimate strength and the thickness ratio parameter.

The burst-pressure data and the empirical burst-pressure equation for each material are plotted in figure 9. In general, the burst data are more consistent at the lower levels of absolute material thickness. A possible explanation is that the thinner diaphragms act more nearly as a membrane. Seventy-two percent of the burst-pressure data falls within ±10 percent of the empirical curves. This percent error was computed by dividing the difference between the experimental and predicted burst pressures by the experimental burst pressure. Three of the data points deviate more than 25 percent from the empirical curves. All three of them are lower than the predicted value and all but one occurred at the lower pressure rise rates (0.05 and 0.1 MN/m^2-sec). The average errors for AISI 1010 steel, AISI 4130 steel, and AISI 347 stainless steel were 7.15, 8.55, and 8.01 percent, respectively.

Effect of Hardness

In an attempt to reduce the data scatter, the hardness values given in table I were used to adjust the ultimate strengths for each diaphragm. A linear relationship between Rockwell hardness and ultimate strength was assumed for each material. A new set of average K values and polynomial constants were computed based on the adjusted ultimate strengths. Substitution of these new K values into equation (1) along with the adjusted ultimate strength did not improve the data scatter and, in fact, made it worse. Several variations to this approach of adjusting ultimate strength with hardness were tried, but they did not improve the data scatter. Apparently, the major cause of this scatter was not due to hardness.

Opening Times

The experimental opening time was measured as the time from first diaphragm crack until the diaphragm petals touched the cylinder wall. By utilizing the value of K obtained from the burst-pressure data, it was found that diaphragm opening times computed from equation (2a) were approximately one-half the experimental value. Similar results were obtained when the predicted burst pressure was replaced by the actual burst pressure in equation (2). There are at least four factors contributing to this disagreement between predicted and experimental opening times. (1) It was assumed in equation (2) that the diaphragms behaved as four petals freely hinged along their edge during the opening sequence; however, it can be seen from figure 10 that 450 microseconds elapse before the diaphragm shears into four petals. (2) The diaphragm petals have stiffness in bending; therefore, they are not freely hinged. (3) The pressure force acting on the diaphragm petals was not constant as assumed. (4) Back pressure acting on the

petals was not considered. Therefore, a significant part of the opening time is neglected in the theory; and in order to account for this part, equation (2a) is multiplied by 2 for the final form

$$\theta = 2\sqrt{\frac{\pi\rho r^2 t}{4Kt_s\sigma}} \tag{4}$$

The opening-time data and equation (4) are plotted in figure 11 for material ultimate strengths of 517.1, 558.5, and 634.3 MN/m^2.

Only 38 percent of the opening-time data falls within ±10 percent of the empirical curves. Two data points deviate by more than 25 percent from the empirical curves, and they do not coincide with the points showing widely varying burst pressure. The average errors for AISI 1010 steel, AISI 4130 steel, and AISI 347 stainless steel are 23.43, 6.38, and 10.73 percent, respectively.

Final Selection

The diaphragms selected for the five burst pressures are presented in table VI. These diaphragms were selected from the empirical curves in figure 9 with the exception of one which was selected from the data. As indicated in table VI, diaphragms fabricated from AISI 347 stainless steel would have the quickest opening times and would burst over the pressure range of 6.9 to 34.5 MN/m^2. The empirical equations or the curves in figures 9 and 11 may be used to select diaphragms other than those listed; however, the validity of these equations has been established only for steel diaphragms bursting into 30.5-cm-diameter square openings with material ultimate strengths of 517.1, 558.5, and 634.3 MN/m^2, a t_s/t ratio between 0.87 and 1.00, and a pressure range between 3.5 and 34.5 MN/m^2.

Dimensionless Burst Parameter

It is recommended in reference 6 that the burst-pressure data be expressed as a dimensionless parameter

$$\phi = \frac{pr}{t_s S\sigma} \tag{5}$$

where

$$S = \frac{4}{\frac{h}{r} + \frac{r}{h}} \tag{6}$$

It states that ϕ is independent of t_s/t and has an experimental value of approximately 0.86. Included in table I is the maximum center deflection before burst for each diaphragm. These data were inserted in equations (5) and (6) and the values obtained ranged

from 0.427 to 1.067 with an average value of 0.702. However, these diaphragms are thicker and have shallower grooves than those presented in reference 6.

CONCLUSIONS

An experimental investigation has been conducted to measure the bursting pressures and opening times of steel diaphragms bursting into a 30.5-cm-square cross section.

1. The test indicated that grooved diaphragms fabricated from AISI 347 stainless steel with a ratio of diaphragm thickness at groove root to diaphragm thickness (t_s/t) less than 0.96 and thicknesses ranging from 1.6 to 6.4 cm had opening times of the order of 1 millisecond, and would burst with no fragmentation in a pressure range from 6.9 to 34.5 MN/m^2.

2. Diaphragms fabricated from AISI 1010 and AISI 4130 steel with t_s/t ratios less than 0.96 burst with no fragmentation but had longer opening times.

3. An opening bend radius of three times the diaphragm thickness was sufficient to prevent the petals from shearing off at their bases.

4. Insufficient data were obtained to determine the effects of pressure rise rate on diaphragm bursting characteristics.

5. Seventy-two percent of the burst-pressure data and thirty-eight percent of the opening-time data fell within ±10 percent of the design equations; however, the validity of these equations for other diaphragm configurations, sizes, or materials has not been established.

6. Adjustment of the data for material hardness did not improve the scatter; in fact, it made it worse.

7. Substitution of the diaphragm data into the equation developed by Edwards (Aeronaut. J., vol. 74, no. 709, Jan. 1970) did not yield the predicted results; however, these diaphragms were thicker and had shallower grooves than those presented by him.

Langley Research Center,
National Aeronautics and Space Administration,
Hampton, Va., April 5, 1972.

APPENDIX

DISCUSSION OF EQUATIONS (1) AND (2)

The theoretical equation for the burst pressure of a plain diaphragm deflecting into a hemispherical shape before rupture is

$$p = \frac{2t\sigma}{r_o} \tag{A1}$$

However, the diaphragms in this investigation were grooved, and also they burst before assuming a hemispherical shape; therefore, an adjustment must be made to the equation. It was decided to replace the factor 2 in equation (A1) with an empirically determined constant which, after a study of the experimental data, was chosen to be a function of the ratio t_s/t. The constant K was determined for each plain or grooved diaphragm tested by inserting the data in equation (1). From these data an average K was determined for each material for t_s/t values of 1.00, 0.95, 0.91, and 0.87 and a least-squares polynomial fit of these average values yielded a third-degree polynomial equation of the form

$$K = \left[C_3(t_s/t)^3 + C_2(t_s/t)^2 + C_1(t_s/t) + C_0\right] \tag{A2}$$

The values of C_3, C_2, C_1, and C_0 for each material are given in table IV.

The opening-time equation (eq. (2)) was based on an analysis such as that given by Drewry and Walenta in reference 3, for instance. It was assumed that the diaphragms behaved during the opening sequence as four freely hinged, triangular petals. The opening time was determined by equating the torque exerted by a constant-pressure force acting on each petal to the product of the petal moment of inertia and the constant angular acceleration which could be expressed in terms of time and angular displacement. This assumption of a constant-pressure force acting on each petal was used in reference 4. However, contrary to both Drewry and Simpson, it was assumed that the diaphragm petals only open through an angle of 45^o since the petals deflect approximately 45^o before rupture.

REFERENCES

1. Rast, J. J.: The Design of Flat-Scored High-Pressure Diaphragms for Use in Shock Tunnels and Gas Guns. NAVORD Rep. 6865, U.S. Navy, Jan. 1961.

2. Armstrong, A. J.; and Watson, R.: Bursting Characteristics of Thin Metal Diaphragms in Shock Tubes. Paper No. 65-WA/Met-16, Amer. Soc. Mech. Eng., 1965.

3. Drewry, J. E.; and Walenta, Z. A.: Determination of Diaphragm Opening-Times and Use of Diaphragm Particle Traps in a Hypersonic Shock Tube. UTIAS Tech. Note No. 90, Inst. Aerosp. Studies, Univ. of Toronto, June 1965.

4. Simpson, C. J. S. M.; Chandler, T. R. D.; and Bridgeman, K. B.: Measurement of Opening Times of Diaphragms in a Shock Tube and the Effect of the Opening Process on Shock Trajectories. NPL Aero Rep. 1194, Brit. A.R.C., May 1966.

5. Cheng, Dah Yu; Dannenberg, Robert E.; and Stephens, Walter E.: A Novel Use of a Telescope To Photograph Metal Diaphragm Openings. AIAA J., vol. 7, no. 6, June 1969, pp. 1209-1211.

6. Edwards, D. G.: The Bursting Pressure of Metal Diaphragms in Square Section Shock Tubes. Aeronaut. J., vol. 74, no. 709, Jan. 1970, pp. 57-58.

TABLE I.- EXPERIMENTAL DATA FOR PLAIN AND GROOVED DIAPHRAGMS

Plate thickness, mm	Groove depth, mm	Minimum thickness / Maximum thickness' percent	Burst pressure, MN/m^2	Opening time, μsec	Pressure rise rate, MN/m^2-sec	Hardness, R_B	Groove type (a)	Maximum diaphragm deflections, h, cm
AISI 1010 steel								
1.52	0.13	92	4.5	1250	131.00	58	RS1	5.7
1.57	0	100	4.3	----	.05	60	P	10.8
2.29	.25	89	5.9	1130	124.11	58	RS1	5.1
2.31	.20	91	5.2	----	.10	45	WS	6.4
2.31	.08	97	6.9	----	.10	46	WS	9.5
2.39	.18	93	7.6	880	172.37	61	RS1	7.0
2.39	.18	93	8.3	500	172.37	61	RS2	5.1
2.39	.18	93	7.6	1020	172.37	61	RS4	4.8
2.39	.20	91	8.3	1100	96.53	60	RS8	5.1
2.41	0	100	7.8	----	.05	60	P	10.2
2.44	.15	94	8.3	930	124.11	63	RS6	4.4
2.44	.13	95	8.3	980	20.00	63	RS1	6.7
2.44	.13	95	7.2	980	68.95	62	RS1	6.7
2.44	.13	95	7.6	960	86.18	62	RS1	6.7
2.44	.15	94	8.3	930	124.11	63	RS1	7.3
2.44	.25	90	6.2	----	.05	60	RS1	6.4
3.02	0	100	9.5	----	.05	50	P	11.4
3.02	.38	87	5.0	850	.05	49	RS1	4.8
3.02	.38	87	5.2	----	34.47	48	RS1	5.1
3.15	.25	92	9.2	----	.05	50	RS1	8.9
3.18	0	100	9.2	----	.05	49	P	9.5
3.18	.13	96	10.3	1030	144.79	48	RS1	8.3
3.18	.25	94	10.3	960	344.74	50	RS1	8.9
5.21	.46	91	13.8	----	.10	68	RS1	6.4
5.59	.25	95	17.2	----	.10	69	RS1	6.4
6.50	.38	94	20.7	----	.10	73	RS1	7.0
Annealed AISI 4130 steel								
3.18	0.25	92	9.7	----	0.10	85	RS1	3.8
3.18	.25	92	8.3	----	.10	97	RS1	2.9
4.75	.13	97	22.1	----	.10	84	RS1	8.9
4.75	.25	95	13.8	1250	.05	81	RS1	5.1
4.78	0	100	22.1	----	.10	83	P	10.2
4.80	.46	90	11.7	----	.10	95	RS1	3.5
4.83	.20	96	21.4	930	413.69	78	RS1	7.3
4.83	.23	95	18.6	----	.10	80	RS1	7.0
4.83	.25	95	19.3	----	.10	82	RS1	7.0
4.83	.23	95	20.7	980	486.63	80	RS1	6.0
4.83	.43	91	15.9	----	.10	91	RS1	4.4
4.85	.33	93	17.2	1000	.10	91	RS1	4.8
4.85	.66	86	13.8	1060	.10	85	RS1	----
Normalized AISI 4130 steel								
3.18	0.13	96	12.1	----	0.05	98	RS1	5.1
6.73	.64	91	22.8	----	.10	99	RS1	4.1
6.73	1.02	85	13.8	----	.10	94	RS1	3.0
AISI 347 stainless steel								
1.52	0.13	92	7.6	----	0.05	76	RS1	8.3
1.52	.13	92	7.6	1000	15.31	77	RS1	7.0
1.52	.15	90	6.9	500	110.32	75	WS	5.7
1.52	.20	87	7.6	----	.10	73	RS1	8.9
1.57	.20	87	6.6	1130	124.11	82	RS1	6.0
1.57	.25	84	5.2	----	.05	76	RS1	7.6
1.68	0	100	8.6	----	.05	75	P	11.4
2.34	0	100	12.1	1000	.05	80	P	10.2
2.36	0	100	12.1	----	.05	79	P	10.2
2.44	.36	85	11.0	930	206.84	81	RS1	7.0
3.00	.25	92	12.4	----	.10	83	RS1	7.6
3.00	.30	90	14.5	1000	48.26	83	RS1	6.4
3.07	.13	95	15.2	1000	193.05	82	RS1	7.3
3.12	.13	96	15.2	----	.10	83	RS1	10.2
3.12	.18	95	15.2	940	241.32	83	RS1	8.3
3.12	.18	95	15.9	1000	241.32	83	RS2	7.0
3.12	.20	94	15.9	960	72.40	82	RS4	6.7
3.12	.25	92	15.9	960	96.53	83	RS8	7.0
3.12	.38	88	11.7	1050	51.71	82	RS1	6.4
3.18	0	100	16.5	----	.05	83	P	10.8
3.18	.25	92	14.5	----	.10	83	RS1	8.3
3.18	.25	92	17.2	820	27.58	86	RS1	10.8
3.18	.28	91	14.5	770	68.95	85	RS1	8.3
3.18	.28	91	15.2	800	68.95	85	RS6	6.7
5.28	2.16	88	24.1	810	413.69	87	RS1	6.4
5.31	.23	96	28.3	880	310.26	87	RS1	9.2
5.38	0	100	28.3	----	.10	83	P	12.7
5.49	.33	94	26.2	----	.10	87	RS1	8.6
6.35	.46	93	26.9	----	.10	83	RS1	10.2
6.35	.64	90	24.8	----	.10	83	RS1	7.0
6.43	.33	95	34.5	925	262.00	85	RS1	8.9
6.58	.33	95	33.1	1090	82.74	82	RS1	8.6
6.60	.46	93	22.8	----	.10	89	RS1	6.7
6.60	1.02	85	17.2	----	.10	87	RS1	5.1
6.68	.89	87	22.1	960	413.69	81	RS1	5.7

[a]Grooved types are designated as follows:

RS1 grooved diaphragm with 0.01 groove root radius
P plain diaphragm
WS wide grooved diaphragm
RS2 grooved diaphragm with 0.02 groove root radius
RS4 grooved diaphragm with 0.04 groove root radius
RS8 grooved diaphragm with 0.08 groove root radius
RS6 grooved diaphragm with 0.06 groove root radius

TABLE II.- BURST PRESSURE FOR DIAPHRAGMS WITH VARYING GROOVE ROOT RADII

Groove root radius, mm	Burst pressure, MN/m^2	$\frac{\text{Minimum thickness}}{\text{Maximum thickness}}$, percent	Plate thickness, mm	Hardness, R_B
AISI 1010 steel				
0.25	8.3	94	2.44	63
.50	7.6	93	2.39	61
1.00	7.6	93	2.39	61
2.00	8.3	91	2.39	60
AISI 347 stainless steel				
0.25	15.2	95	3.12	83
1.00	15.9	94	3.12	82
.75	15.2	91	3.12	85
2.00	15.9	92	3.12	83

TABLE III.- COMPARISON OF OPENING TIMES FOR KNIFE-SHEARED AND GROOVED DIAPHRAGMS

Burst mode	Plate thickness, mm	$\frac{\text{Minimum thickness}}{\text{Maximum thickness}}$, percent	Burst pressure, MN/m^2	Pressure rise rate, MN/m^2-sec	Opening time, μsec
AISI 1010 steel					
Knife	2.24		5.2	0.05	----
Knife	2.24		5.5	.05	----
Knife	2.26		5.5	.05	----
Knife	2.31		5.2	6.90	2090
Groove	3.02	87	5.0	.05	850
Knife	2.31		5.9	34.47	1300
Groove	2.29	89	5.9	124.11	1130
Knife	2.41		8.6	137.90	1300
Groove	2.41	95	8.3	20.00	980
Groove	2.44	94	8.3	124.11	930
Knife	2.44		6.9	10.34	1700
Groove	2.44	95	7.2	68.75	980
Knife	2.46		7.6	9.65	1050
Groove	2.39	93	7.6	172.37	880
Groove	2.44	95	7.6	86.18	960
Knife	3.15		9.0	27.58	700
AISI 347 stainless steel					
Knife	1.57		6.9	20.68	900
Groove	1.57	87	6.6	124.11	1130
Knife	1.57		7.9	.10	980
Groove	1.52	92	7.6	15.31	1000

TABLE IV.- CONSTANTS FOR EQUATION FOR K

Material	C_3	C_2	C_1	C_0
AISI 1010 steel	332.03	-976.77	956.79	-311.14
AISI 4130 steel	-938.39	2620.09	-2430.38	749.99
AISI 347 stainless steel	-35.34	95.64	-85.84	26.82

TABLE V.- AVERAGE K COMPUTED FROM DATA

Material	K value for t_s/t of –			
	1.00	0.95	0.91	0.87
AISI 1010 steel	0.91	0.96	0.90	0.56
AISI 4130 steel	1.32	1.20	.88	.79
AISI 347 stainless steel	1.28	1.29	1.27	1.21

TABLE VI. - DIAPHRAGMS SELECTED FOR FIVE BURST PRESSURES

Burst pressure, MN/m^2	Plate thickness, mm	$\frac{\text{Minimum thickness}}{\text{Maximum thickness}}$, percent	Opening time, μsec	Material
6.9	1.60	85	940	AISI 347 stainless steel
	1.60	96	920	AISI 4130 steel
	2.39	91	1150	AISI 1010 steel
13.8	3.18	85	940	AISI 347 stainless steel
	3.18	96	920	AISI 4130 steel
	4.78	91	1160	AISI 1010 steel
20.7	3.96	96	850	AISI 347 stainless steel
	4.78	96	920	AISI 4130 steel
27.6	6.35	96	920	AISI 347 stainless steel
	5.56	93	870	AISI 4130 steel
34.5	6.35	95	860	AISI 347 stainless steel

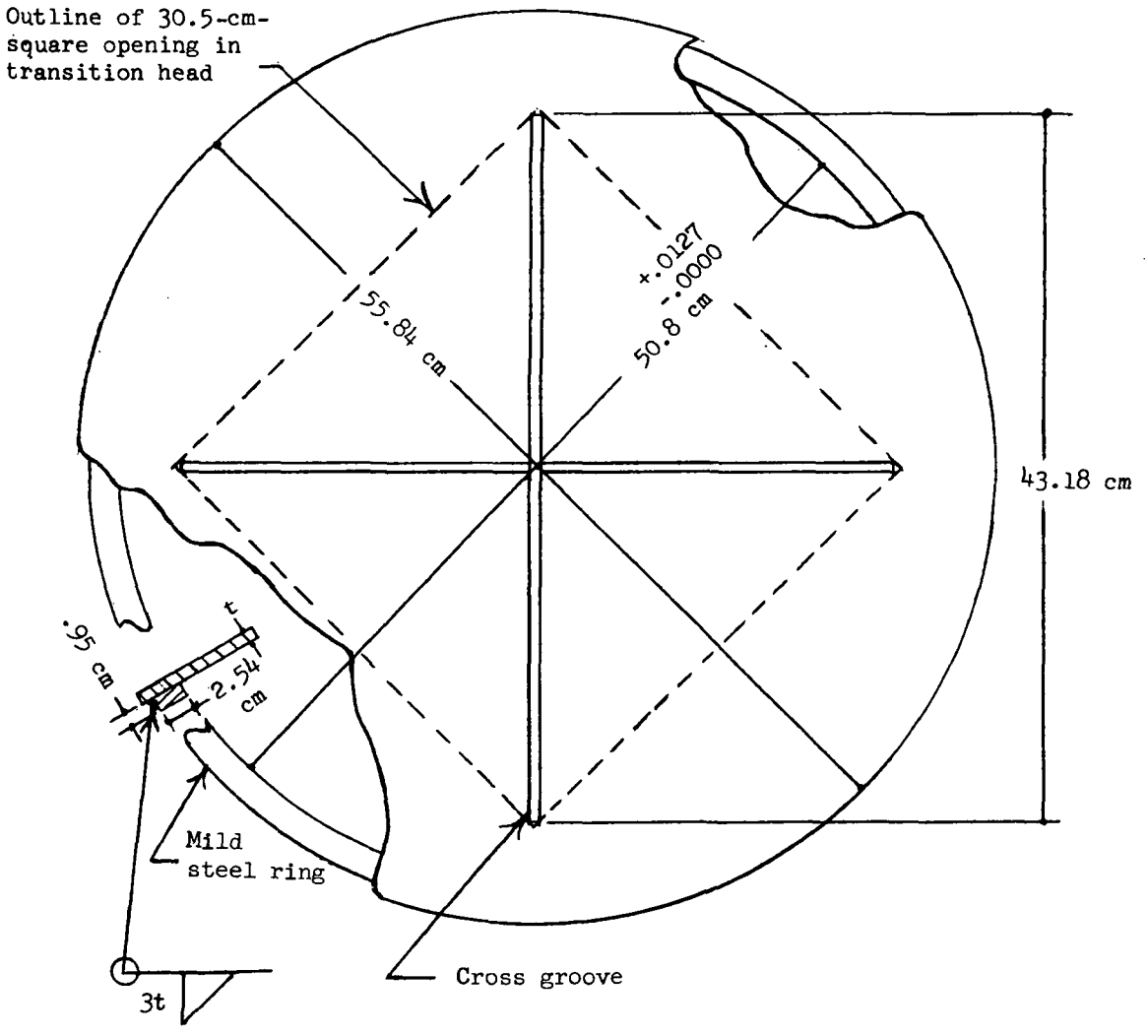

Figure 1.- Typical test diaphragm. Diaphragm materials: AISI 1010, 4130, and 347 steel.

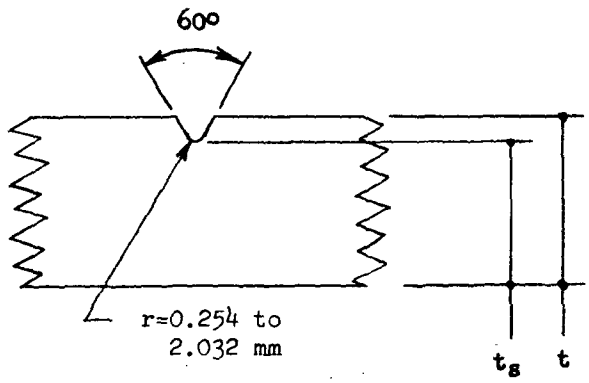

V-Groove

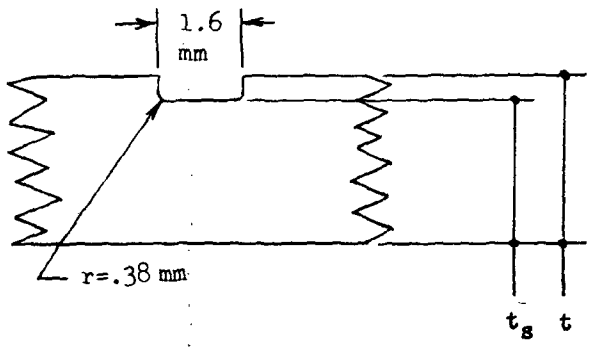

Wide groove

Figure 2.- Groove geometries.

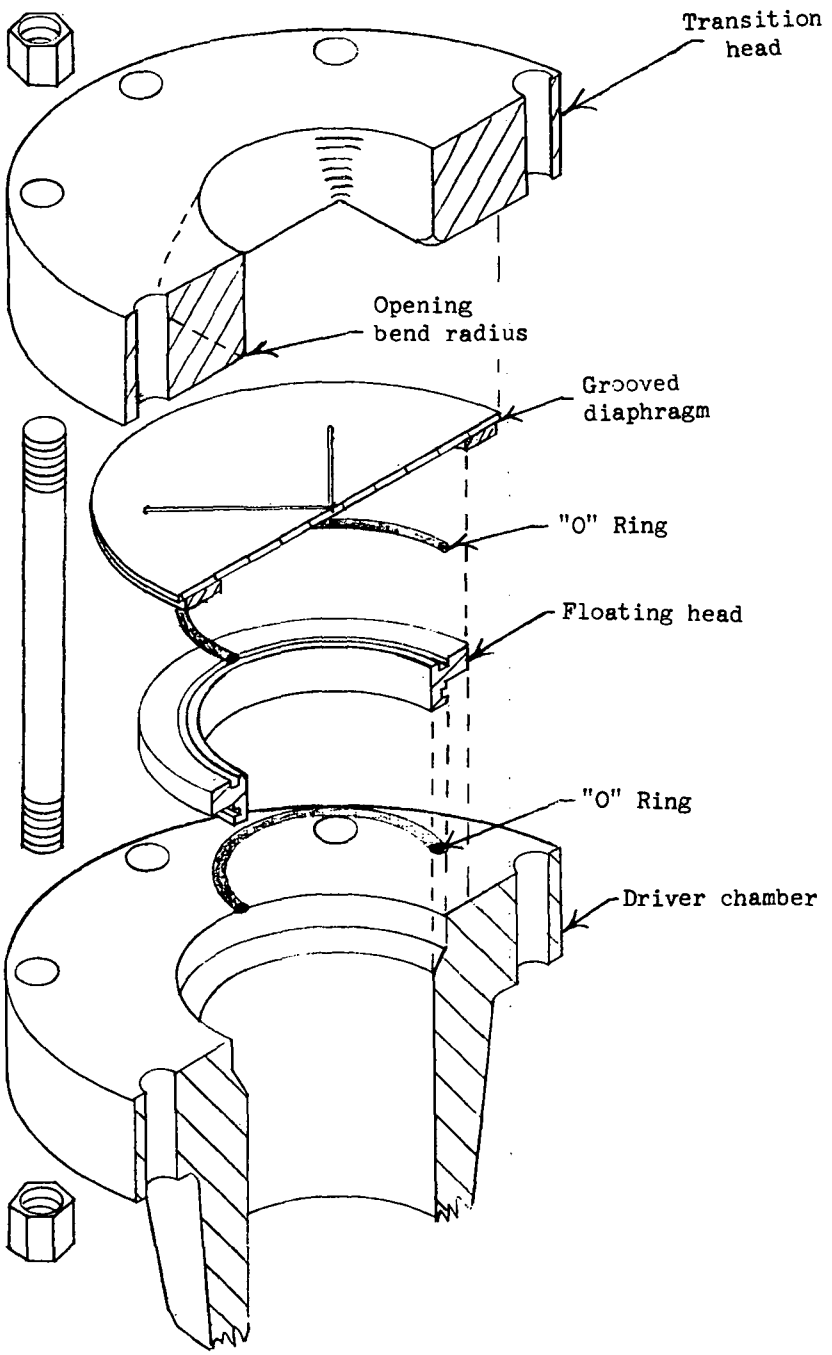

Figure 3.- Exploded assembly of diaphragm clamping arrangement.

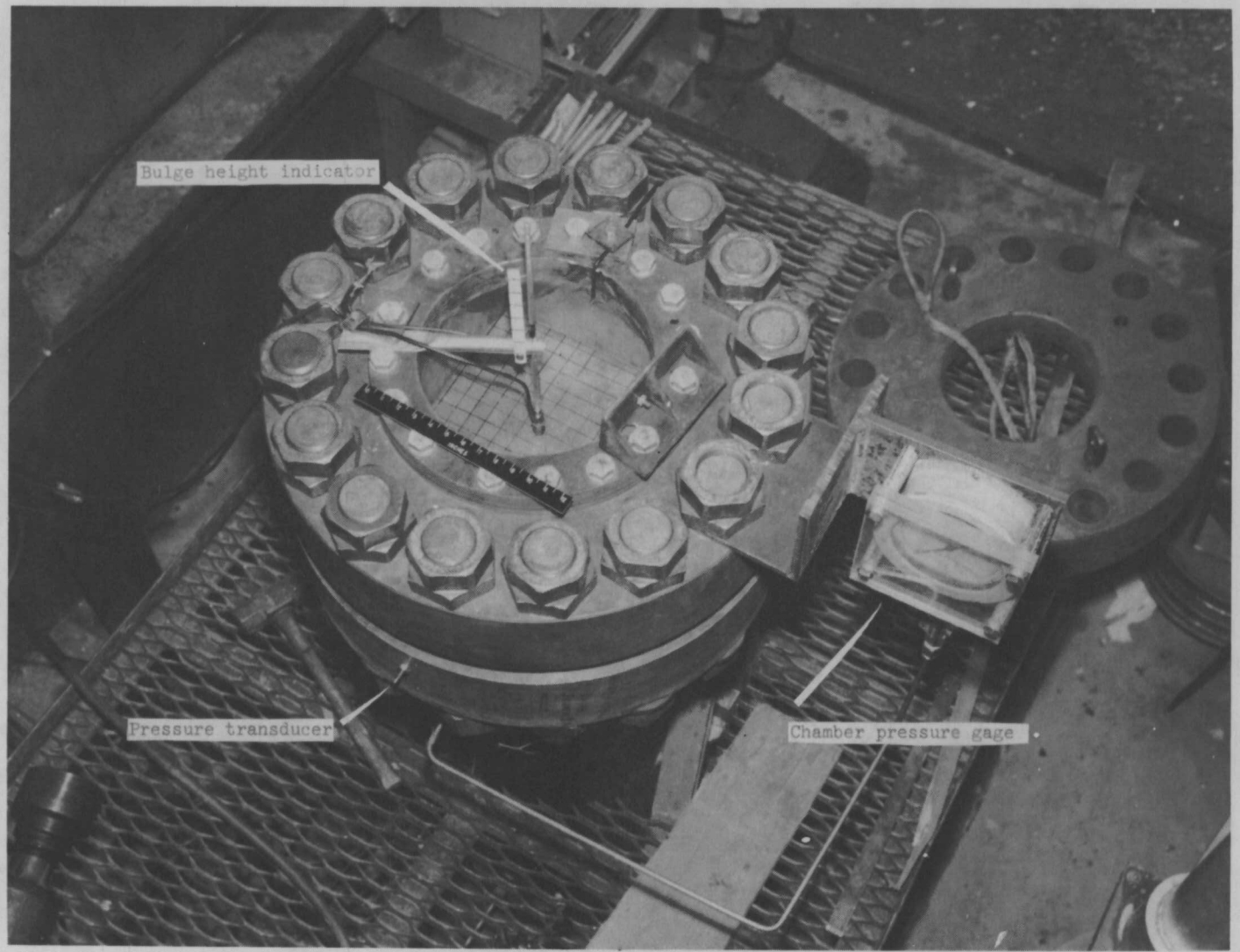

L-65-2904.1

Figure 4.- Instrumentation for pressure rise rates between 0.05 and 0.1 MN/m^2-sec.

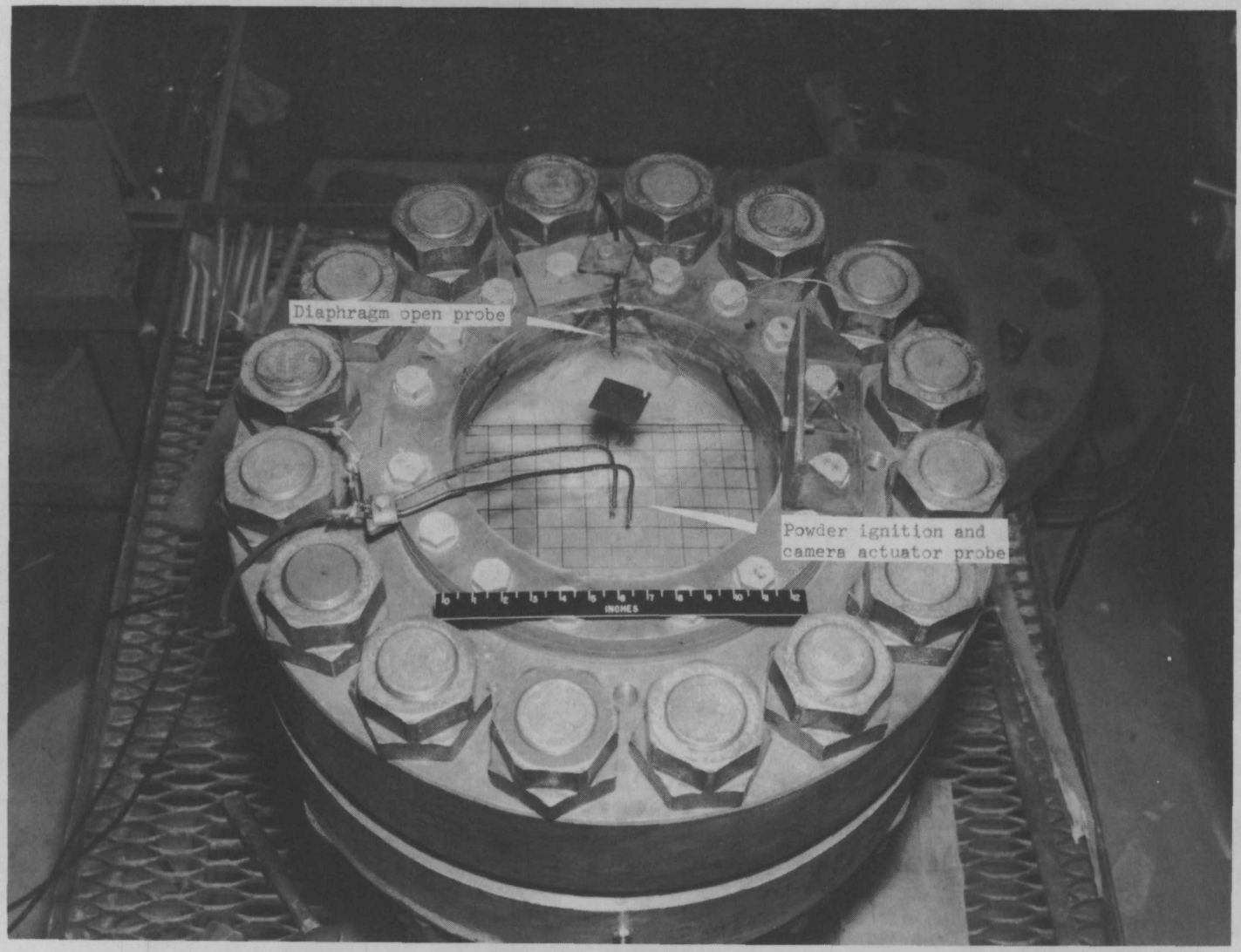

L-65-2905.1

Figure 5.- Instrumentation for pressure rise rates between 0.1 and 483 MN/m^2-sec.

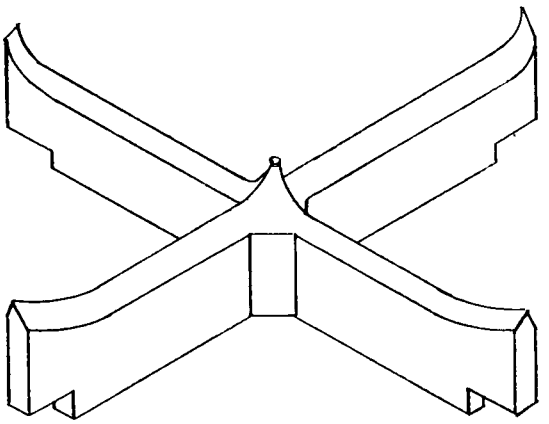

Figure 6.- Knife.

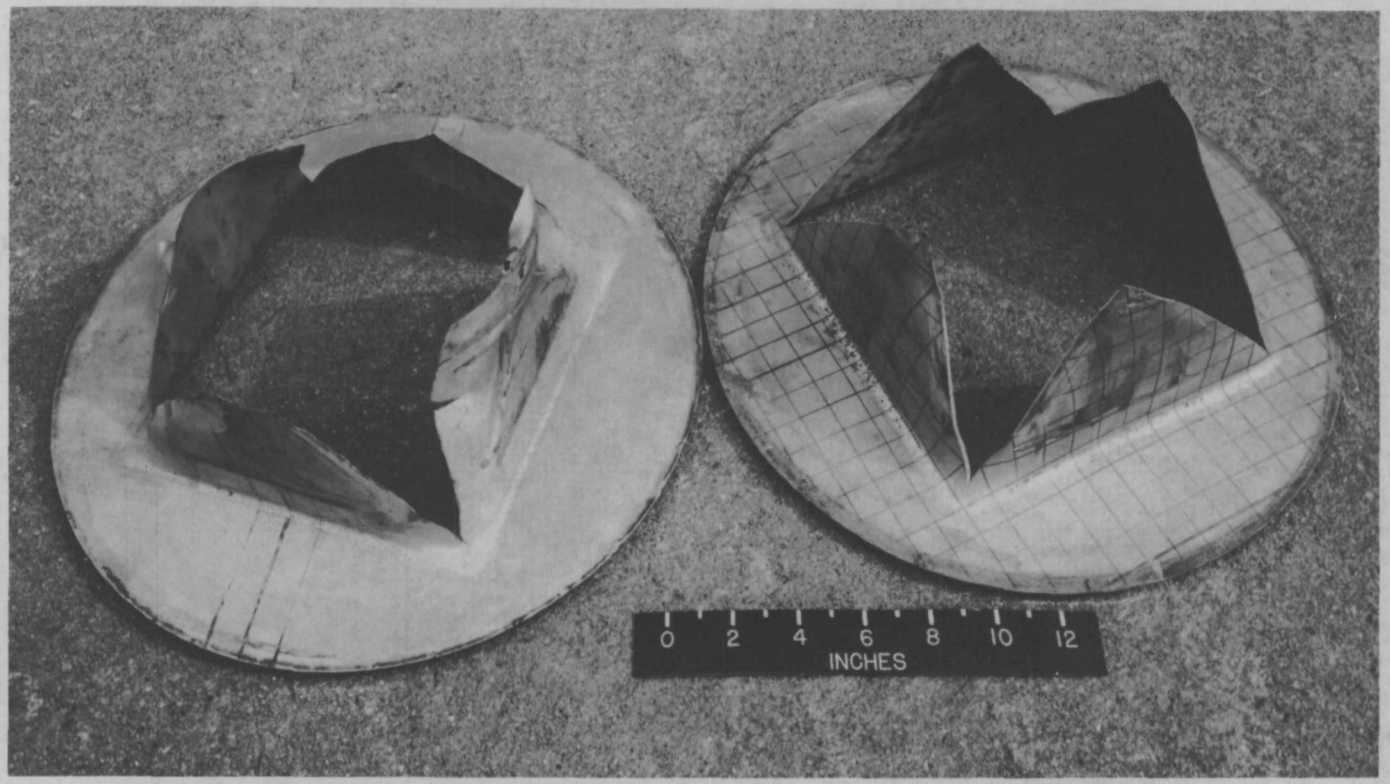

Material: AISI 347 stainless steel
Thickness: 1.68 mm
t_s/t: 1.00
Pressure rise rate: 0.05 MN/m^2-sec
Burst pressure: 8.6 MN/m^2

Material: AISI 347 stainless steel
Thickness: 3.124 mm
t_s/t: .88
Pressure rise rate: 52 MN/m^2-sec
Burst pressure: 11.7 MN/m^2

L-67-5825.1

Figure 7.- Comparison of break characteristics of grooved and plain diaphragms.

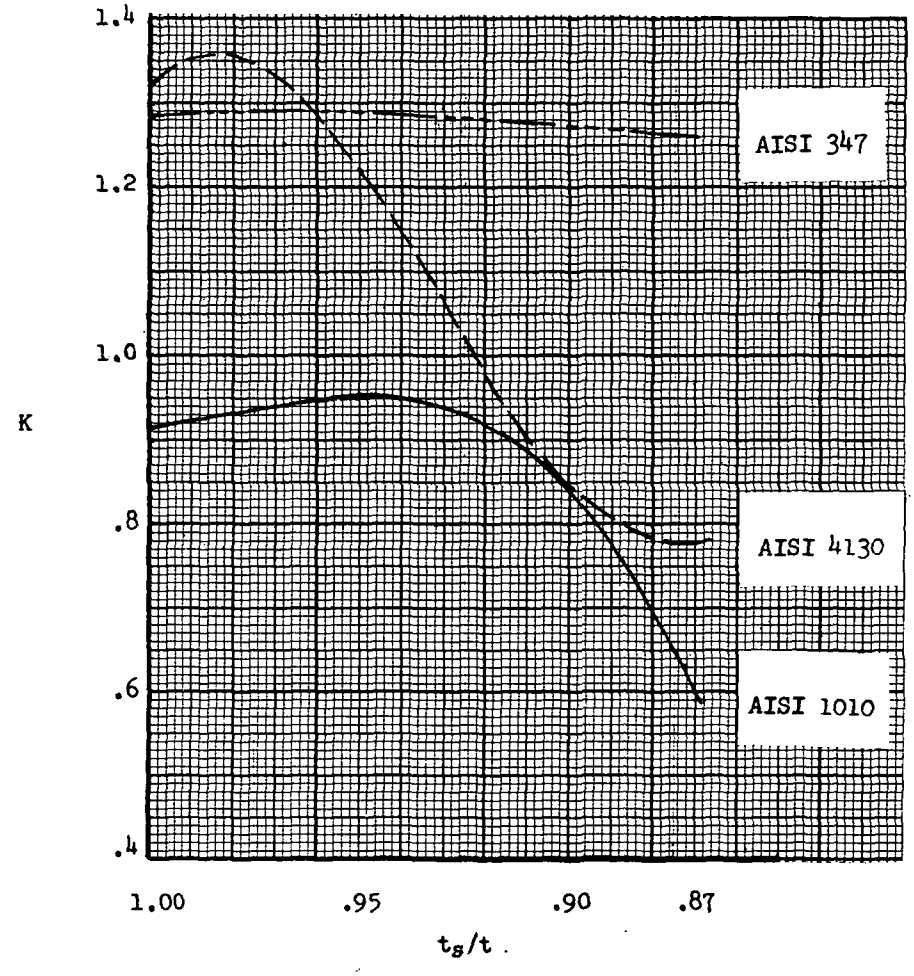

Figure 8.- Empirical constant K. r = 15.2 cm; r_s = 0.25 mm.

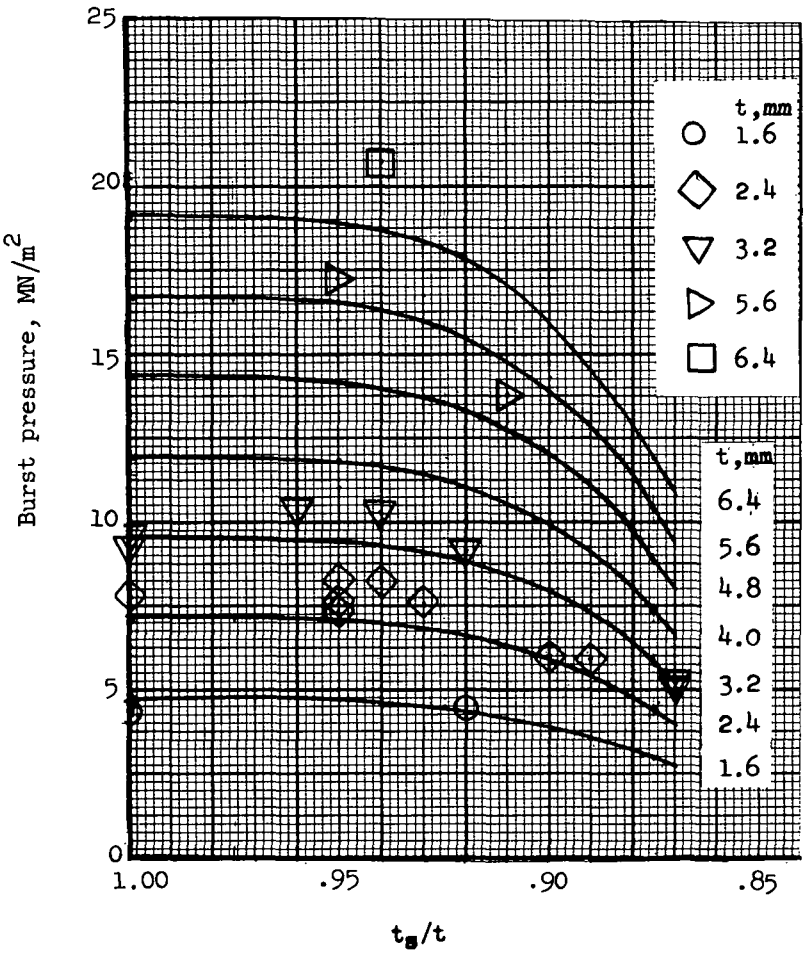

(a) AISI 1010 steel; σ = 517 MN/m^2.

Figure 9.- Predicted burst pressures for grooved diaphragms compared with experimental data. r = 15.2 cm; r_s = 0.25 mm.

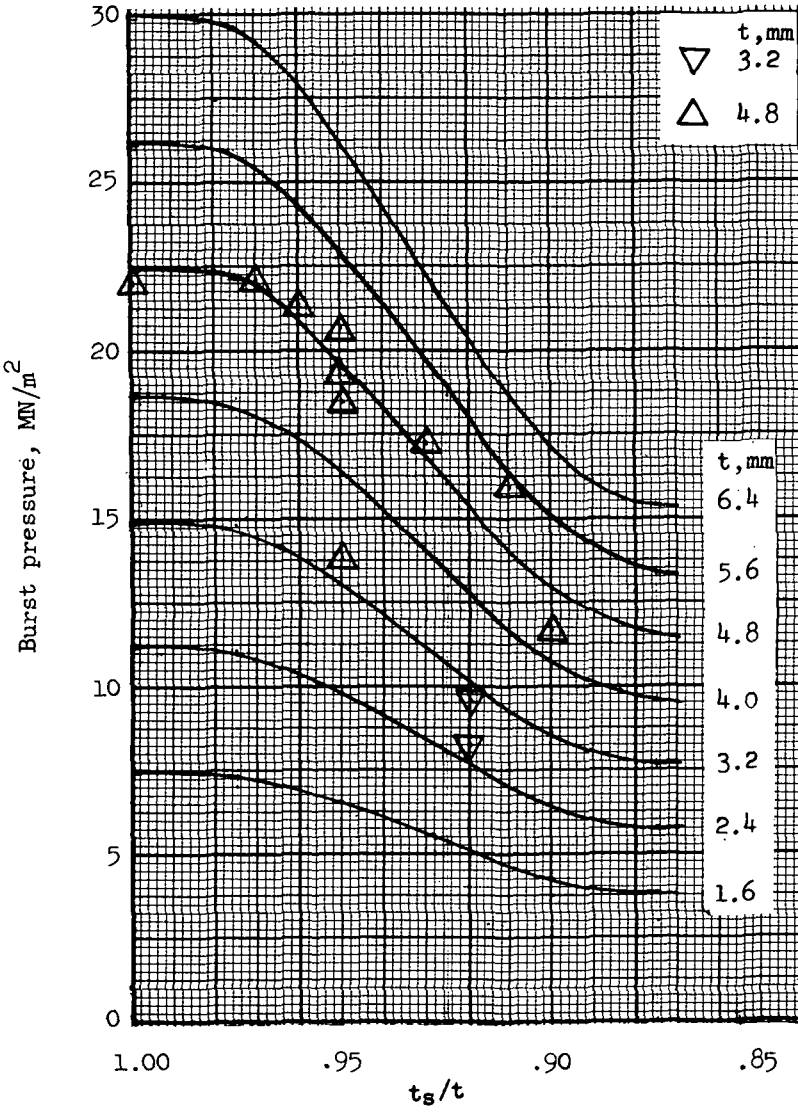

(b) AISI 4130 steel; $\sigma = 558$ MN/m^2.

Figure 9.- Continued.

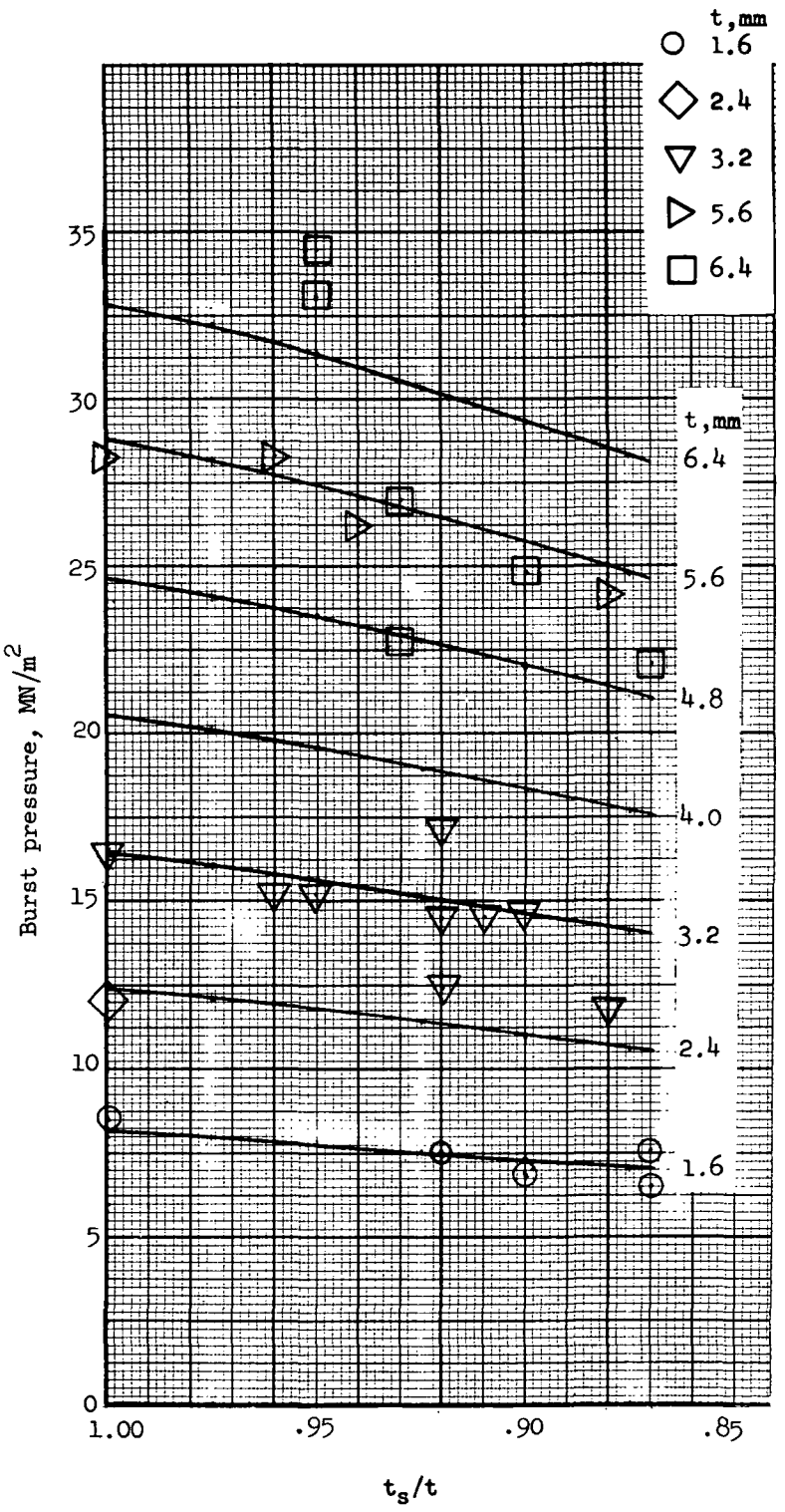

(c) AISI 347 stainless steel; $\sigma = 634$ MN/m^2.

Figure 9.- Concluded.

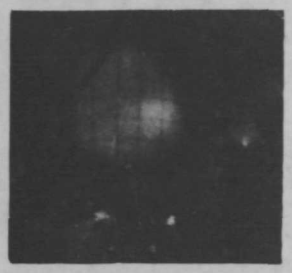

FRAME 1
Time: 0 microseconds

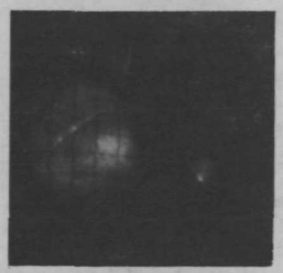

FRAME 2
Time: 150 microseconds

FRAME 3
Time: 300 microseconds

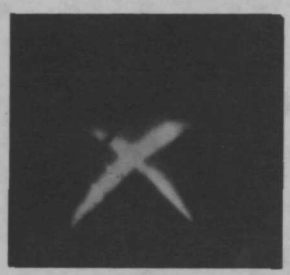

FRAME 4
Time: 450 microseconds

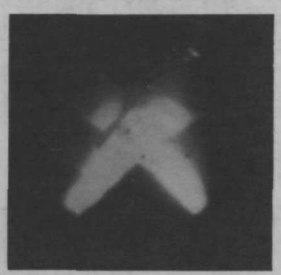

FRAME 5
Time: 600 microseconds

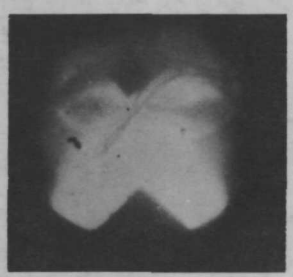

FRAME 6
Time: 750 microseconds

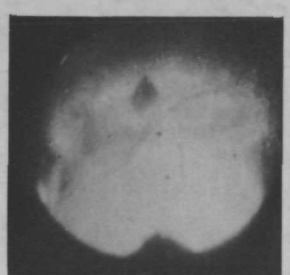

FRAME 7
Time: 900 microseconds

FRAME 8
Time: 1050 microseconds

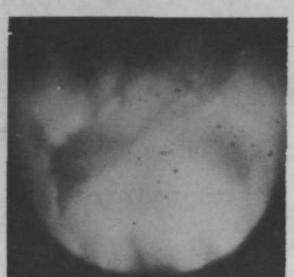

FRAME 9
Time: 1200 microseconds

L-72-2411

Figure 10.- High-speed sequence photograph of diaphragm burst. $t = 1.524$ mm; $\frac{t_s}{t} = 0.92$; $p = 7.584$ MN/m^2; AISI 347 stainless steel.

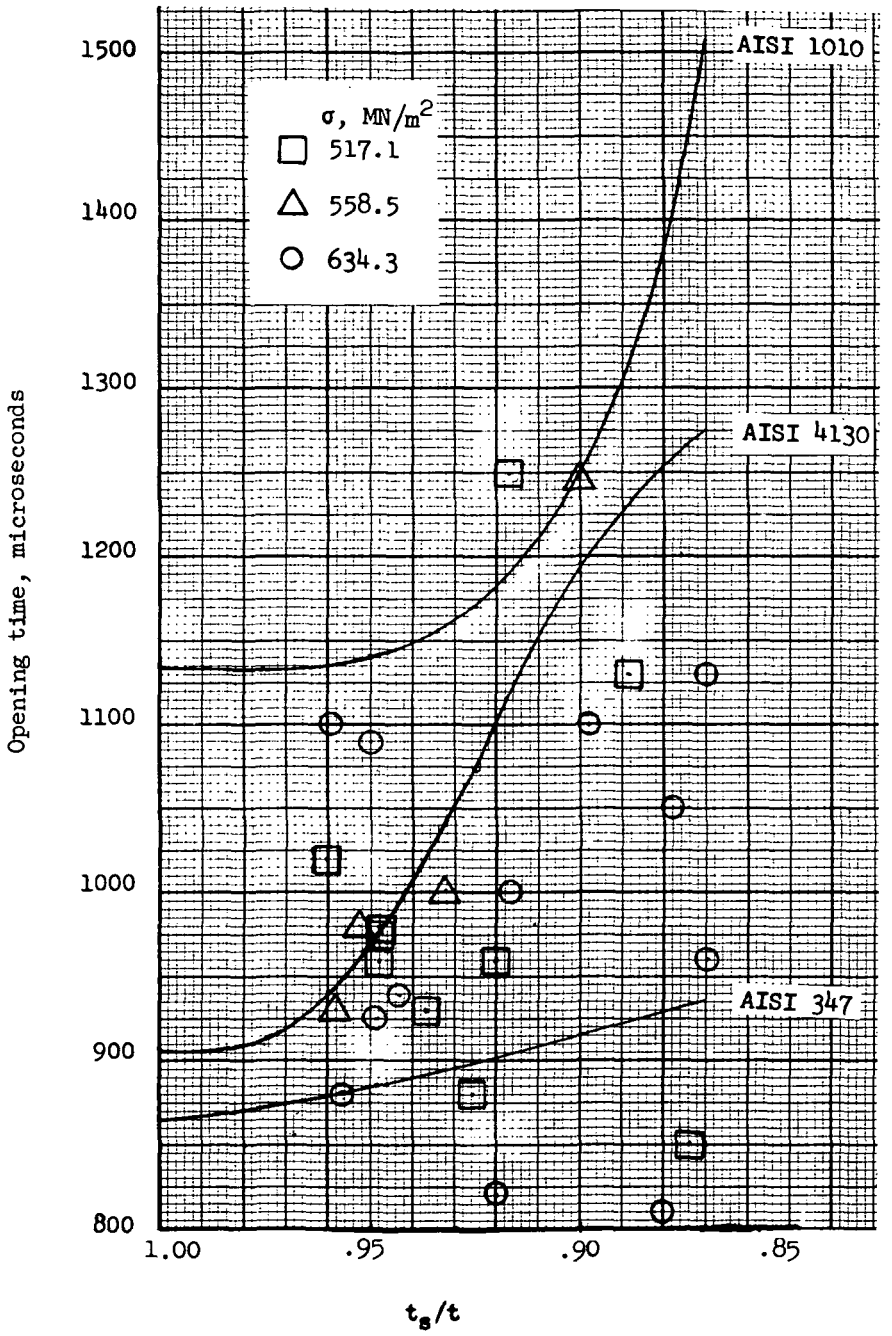

Figure 11.- Predicted opening times for scribed diaphragms compared with experimental data. r = 15.2 cm; r_s = 0.25 mm.

"The aeronautical and space activities of the United States shall be conducted so as to contribute . . . to the expansion of human knowledge of phenomena in the atmosphere and space. The Administration shall provide for the widest practicable and appropriate dissemination of information concerning its activities and the results thereof."

—NATIONAL AERONAUTICS AND SPACE ACT OF 1958

NASA SCIENTIFIC AND TECHNICAL PUBLICATIONS

TECHNICAL REPORTS: Scientific and technical information considered important, complete, and a lasting contribution to existing knowledge.

TECHNICAL NOTES: Information less broad in scope but nevertheless of importance as a contribution to existing knowledge.

TECHNICAL MEMORANDUMS: Information receiving limited distribution because of preliminary data, security classification, or other reasons.

CONTRACTOR REPORTS: Scientific and technical information generated under a NASA contract or grant and considered an important contribution to existing knowledge.

TECHNICAL TRANSLATIONS: Information published in a foreign language considered to merit NASA distribution in English.

SPECIAL PUBLICATIONS: Information derived from or of value to NASA activities. Publications include conference proceedings, monographs, data compilations, handbooks, sourcebooks, and special bibliographies.

TECHNOLOGY UTILIZATION PUBLICATIONS: Information on technology used by NASA that may be of particular interest in commercial and other non-aerospace applications. Publications include Tech Briefs, Technology Utilization Reports and Technology Surveys.

Details on the availability of these publications may be obtained from:

SCIENTIFIC AND TECHNICAL INFORMATION OFFICE

NATIONAL AERONAUTICS AND SPACE ADMINISTRATION

Washington, D.C. 20546